Isotopes in Environmental and Health Studies
Vol. 42, No. 1, March 2006, 21–35

Taylor & Francis
Taylor & Francis Group

Applications of cavity ring-down spectroscopy to high precision isotope ratio measurement of $^{13}C/^{12}C$ in carbon dioxide

ED H. WAHL†, BERNARD FIDRIC†, CHRIS W. RELLA†, SERGEI KOULIKOV†, BORIS KHARLAMOV†, SZE TAN†, ALEXANDER A. KACHANOV†, BRUCE A. RICHMAN†, ERIC R. CROSSON†, BARBARA A. PALDUS*†, SHASHI KALASKAR‡ and DAVID R. BOWLING‡

†Picarro Inc., 480 Oakmead Parkway, Sunnyvale, CA 94085, USA
‡Department of Biology, University of Utah, 257 S 1400 E, Salt Lake City, UT 84112, USA

(Received 10 January 2005; in final form 16 July 2005)

Recent measurements of carbon isotopes in carbon dioxide using near-infrared, diode-laser-based cavity ring-down spectroscopy (CRDS) are presented. The CRDS system achieved good precision, often better than 0.2‰, for 4 % CO_2 concentrations, and also achieved 0.15–0.25‰ precision in a 78 min measurement time with cryotrap-based pre-concentration of ambient CO_2 concentrations (360 ppmv). These results were obtained with a CRDS system possessing a data rate of 40 ring-downs per second and a loss measurement of $4.0 \times 10^{-11}\,cm^{-1}\,Hz^{-1/2}$. Subsequently, the measurement time has been reduced to under 10 min. This standard of performance would enable a variety of high concentration (3–10 %) isotopic measurements, such as medical human breath analysis or animal breath experiments. The extension of this ring-down to the 2 μm region would enable isotopic analysis at ambient concentrations, which, combined with the small size, robust design, and potential for frequent measurements at a remote site, make CRDS technology attractive for remote atmospheric measurement applications.

Keywords: Atmosphere; Carbon dioxide; Carbon-12; Carbon-13; Cavity ring-down spectroscopy; Infrared diode laser

1. Introduction

For scientists, stable isotope analysis of atmospheric CO_2 [1] and biospheric–atmospheric CO_2 [2] exchange (both carbon and oxygen isotopes) offer the unique opportunity to assess ecosystem physiology (exchange between soils [3], vegetation [4], and the atmosphere [5]), to determine the origin and partitioning of net ecosystem CO_2 fluxes [6] (*e.g.* respiration, photosynthesis, and assimilation), and to identify biospheric imprints onto the atmosphere [7]

*Corresponding author. Skymoon Ventures, 3045 Park Boulevard, Palo Alto, CA 94036, USA. Tel.: +1-408-203-8560; Fax: +1-650-688-3119; Email: barbara@skymoonventures.com

Isotopes in Environmental and Health Studies
ISSN 1025-6016 print/ISSN 1477-2639 online © 2006 Taylor & Francis
http://www.tandf.co.uk/journals
DOI: 10.1080/10256010500502934

(*e.g.* carbon sources and sinks). Operating on time scales ranging from hours to thousands of years, these processes play significant roles not only in biospheric–atmospheric gas exchange, but also in the global carbon cycle as a whole.

The isotope ratio ($^{13}C/^{12}C$) is expressed as a 'delta' ($\delta^{13}C$) compared with an arbitrary standard (Vienna Pee Dee Belemnite, VPDB):

$$\delta^{13}C = \frac{(^{13}C/^{12}C)_{\text{measured}} - (^{13}C/^{12}C)_{\text{VPDB}}}{(^{13}C/^{12}C)_{\text{VPDB}}} \quad (1)$$

This delta value is expressed in parts per million or parts per thousand (‰). The delta of carbon dioxide encountered in ambient air generally varies between about −7 and −13 ‰ (relative to VPDB). The resolution of interest for atmospheric science is about 0.01 to 0.3 ‰. The range in delta that one might encounter in a terrestrial environment is about −50 to +5 ‰. Measurement of the isotopic carbon ratio, $\delta^{13}C$, is distinct from the total carbon dioxide concentration, which is nominally about 370 parts per million by volume (ppmv) in the ambient atmosphere, but can range from 350 to 700 ppmv locally.

Air sample collection methods and isotope ratio mass spectrometry (IRMS) have evolved into a very useful research tool for atmospheric applications since the early studies of Keeling in 1958 [8] and have allowed studies of large-scale short-term and long-term variations in the atmosphere. However, soil and air sampling using IRMS remains a time-consuming process, as does the fact that IRMS is generally not operated in the field, which leads to significant human resources being expended to collect, classify, prepare, and measure samples. As a result, there is a need for smaller, portable, less labour-intensive, and relatively cheaper ($\sim$<$50 K) instruments that can operate in the field and make frequent measurements of both the absolute concentration of CO_2 and its isotopic composition. The ideal desired precision is 0.01 to 0.1 ‰, although this precision may not be required by all applications (some may even be able to use a resolution of 1 ‰). Ideally, an optically-based instrument could operate *in situ* (*e.g.* forest, measurement tower, crop field) for several months with minimal attention.

In this article, we describe an optical absorption instrument based on cavity ring-down spectroscopy (CRDS), a trace detection method that can measure absolute optical loss [9] (see, *e.g.* [9] and references therein). The instrument was developed for high precision measurements of carbon isotope ratios in carbon dioxide (CO_2) and is described in the Experimental setup section of this article. The instrument was tested first at Picarro and subsequently at the University of Utah for performance, reliability, and robustness. The results from these tests are summarized in the Results and analysis section. Finally, a discussion of potential improvements to the instrument for atmospheric measurements is included in the Conclusions section.

2. Cavity ring-down spectroscopy

In optical absorption spectroscopy, a spectral feature called an absorption peak of a target species is measured in order to obtain its concentration. Although different species may absorb light at one or more identical wavelengths, their overall spectral profile, consisting of many absorption peaks, often called a 'fingerprint', is unique. The ability of a spectrometer to distinguish between two different isotopic species that absorb at similar wavelengths is called selectivity. Figure 1 illustrates the high resolution, near-infrared spectrum of CO_2 at 6.7 kPa, which was used in this study to measure the carbon isotopes of CO_2. These spectral features depend on sample pressure and sharpen (decreased spectral width) as the sample pressure is decreased. Therefore, selectivity of isotopic measurements can often be improved by reducing the sample pressure below atmospheric pressure. However, narrower spectral features are

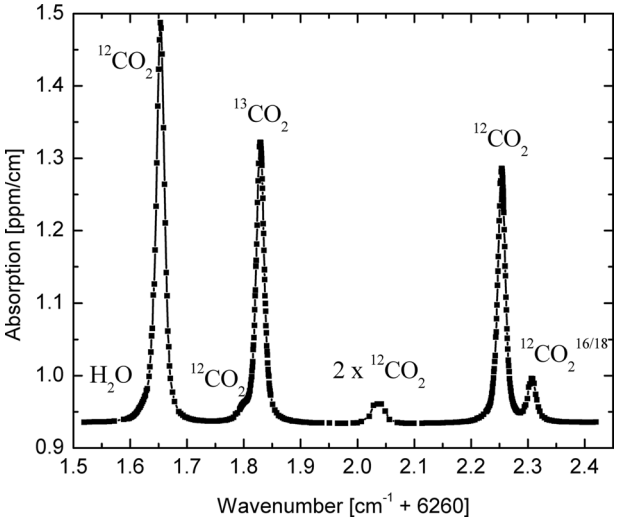

Figure 1. Near-infrared spectrum of 5 % carbon dioxide (CO_2) at 6.7 kPa operating pressure, showing three different isotopes.

more difficult to measure because they require the instrument to distinguish between closely spaced wavelengths of light [10]. Continuous wave (CW) laser systems can show significantly better spectral resolution when measuring absorption features of isotopic species than the incoherent light sources and filters used by non-dispersive infrared (NDIR) systems to measure entire ro-vibrational bands of isotopes. CW lasers are used in tunable diode laser absorption spectroscopy (TDLAS) to achieve high selectivity [10].

The second key performance parameter for measuring isotopes is sensitivity. Sensitivity is often described as the smallest detectable change in 1 cm of path length that a spectrometer can measure during 1 s [11]. If many measurements can be made within 1 s, averaging may be used to further improve (by a factor of the square root of the number of measurements or the square root of the data acquisition rate) the achievable sensitivity [11]. Sensitivity has units of $\mathrm{cm}^{-1}\,\mathrm{Hz}^{-1/2}$ [11]. Sensitivity is a well-established figure of merit for any absorption-based technique. Because laser light has extremely long coherence lengths and can stay collimated to a small beam size over long distances, TDLAS using multi-pass cells can routinely achieve tens of metres of path length enhancement [12]. However, multi-pass cell TDLAS still remains limited by laser intensity fluctuations and interference fringes [12]. Moreover, TDLAS techniques do not provide an absolute optical loss measurement. Despite these limitations, TDLAS has been applied successfully to isotopic absorption measurements of carbon dioxide [12, 13], water [14, 15], methane [16], and nitrous oxide [17].

CRDS is a more recently developed TDLAS approach that replaces a multi-pass cell with a stable optical resonator, often called the ring-down cavity (RDC). CRDS is based on the principle of measuring the rate of decay of light intensity inside the RDC [9] (see, *e.g.* [9] and references therein). Once sufficient light is injected into the RDC from a laser source, the input light is interrupted, and the decay of the stored light transmitted out of the cavity through one of the RDC mirrors is monitored using a photodetector. The transmitted light, $I(t, \lambda)$, from the RDC is given by

$$I(t, \lambda) = I_0 \mathrm{e}^{-t/\tau(\lambda)} \tag{2}$$

where I_0 is the transmitted light at the time the light source is shut off, $\tau(\lambda)$ is the ring-down time constant, and $1/\tau(\lambda)$ is the decay rate. The transmitted light intensity decays exponentially over time. The total (round-trip) optical loss inside the cavity is $L(\lambda) = [c\,\tau(\lambda)]^{-1}$, where c is the speed of light. The total optical loss is comprised of the empty cavity optical loss and the sample optical loss. CRDS provides an absolute measurement of these optical losses. The empty cavity (round-trip) optical loss, $L_{\text{empty}}(\lambda)$, is comprised of the scattering and transmission losses at the mirrors. In general, better mirrors provide lower empty cavity losses and higher sensitivity. The sample (round-trip) optical loss is $A(\lambda) = \alpha(\lambda) l_{\text{rt}}$, where l_{rt} is the cavity round-trip length, and $A(\lambda)$ is simply the difference between total cavity losses and empty cavity losses, namely, $A(\lambda) = L(\lambda) - L_{\text{empty}}(\lambda)$. Once the absorption spectrum, $\alpha(\lambda)$, of the sample has been measured, then the sample concentration can be readily computed using the absorption cross-section and line-shape parameters.

The single-shot measurement uncertainty for a CRDS system is defined by

$$\alpha_{\text{min}} = \frac{(\Delta\tau/\tau)}{l_{\text{eff}}}, \tag{3}$$

where $\Delta\tau/\tau$ is called the shot-to-shot noise of the system. The effective path length of a CRDS measurement is $l_{\text{eff}} = l_{\text{rt}}/L_{\text{empty}}$. For typical RDC mirrors having a reflectivity of 99.995 %, and scattering losses of <0.0005 %, the path length enhancement can exceed 20,000. For a 20 cm long sample cell, the round-trip path length is 40 cm, so that the effective round-trip path length is 8 km. A good CRDS system can achieve a shot-to-shot variation of 0.03 %, leading to a single-shot uncertainty of $3 \times 10^{-10}\,\text{cm}^{-1}$. Note also that the CRDS measurement is not dependent on either the initial intensity of the light inside the cavity, provided the signal has a sufficient signal-to-noise ratio at the detector, or the physical sample path length as in the traditional absorption spectroscopy.

Moreover, CRDS uses laser sources having narrow line widths and providing high spectral resolution, so that a CRDS system can operate at sub-atmospheric pressures to minimize any spectral line overlap for the target species. We also note here that a stable optical RDC can accomplish this sensitivity enhancement for sample volumes as small as 25 ml, compared with traditional NDIR or TDLAS cells, which require volumes of ≥200 ml. CRDS can therefore resolve three typical limitations of near-infrared diode laser-based absorption spectroscopy, namely sensitivity, and dependence on intensity noise of the light source. These advantages of CRDS result directly in improved robustness and reliability of operation for a field deployable instrument.

The use of CRDS for measuring isotopic ratios is not novel. In earlier work, measurements of isotopes in methane [18] and carbon dioxide [19] focused primarily on demonstrating the potential of using CRDS as a laboratory method for isotopic measurement applications. It is important to note that for practical field deployment of any optical technology for isotopic measurements, all optical components must be both commercially available and robust. For TDLAS-based instruments, only telecom grade diode lasers designed to operate in the near-infrared satisfy these conditions.

Hence, the instrument reported here was tailored to utilize near-infrared diode lasers, despite the significantly weaker overtones of the absorption lines compared with mid-infrared ones. This article describes the research performed to better understand the detailed performance, reproducibility, and robustness of near-infrared isotopic CRDS measurements in the context of atmospheric research. Furthermore, the results obtained in this work represent a new performance benchmark for near-infrared CRDS specifically and near-infrared isotopic optical systems in general.

3. Experimental setup

The CRDS instrument was implemented using a triangular ring cavity and a directly modulated distributed feedback (DFB) diode laser source as shown in figure 2. The DFB laser is pigtailed with a polarization-maintaining fibre. This fibre attaches to an etalon-based wavelength monitor that uses only a small fraction of the incident light. Most of the laser light simply passes through the wavelength monitor and is optically isolated before being coupled into the RDC cell. The light leaking out of one of the cavity mirrors is directed to the ring-down detector. The ring-down detector measures cavity power as a function of time. The 14-bit A/D card digitizes the output of the detector. The DSP card analyses the digital output to determine the ring-down time.

The procedure for measuring the spectrum of CO_2 and its isotopologues in the cavity is as follows.

- Set the laser to the starting ($n = 1$) wavelength $\lambda_{n=1}$, which is shorter than the wavelength of the absorption feature of interest.
- Bring the laser and the cavity into resonance by dithering a piezoelectric actuator (PZT) to move one of the cavity's end mirrors, thereby adjusting the cavity length.
- Turn the laser off when sufficient light intensity builds up in the cavity.
- Monitor the detector signal and record the ring-down curve.
- Convert the ring-down time to an absorbance.
- Scan the laser wavelength to λ_{n+1} and repeat the process.

By repeating the process several times over a wavelength range that encompasses the absorption feature, the instrument collects a series of ring-down curves to give a measurement of the absorption spectrum. A 'scan' typically measures the $^{13}CO_2/^{12}CO_2$ isotopic ratio from the absorption spectrum shown in figure 1 (6261.5 to 6262.4 cm^{-1}).

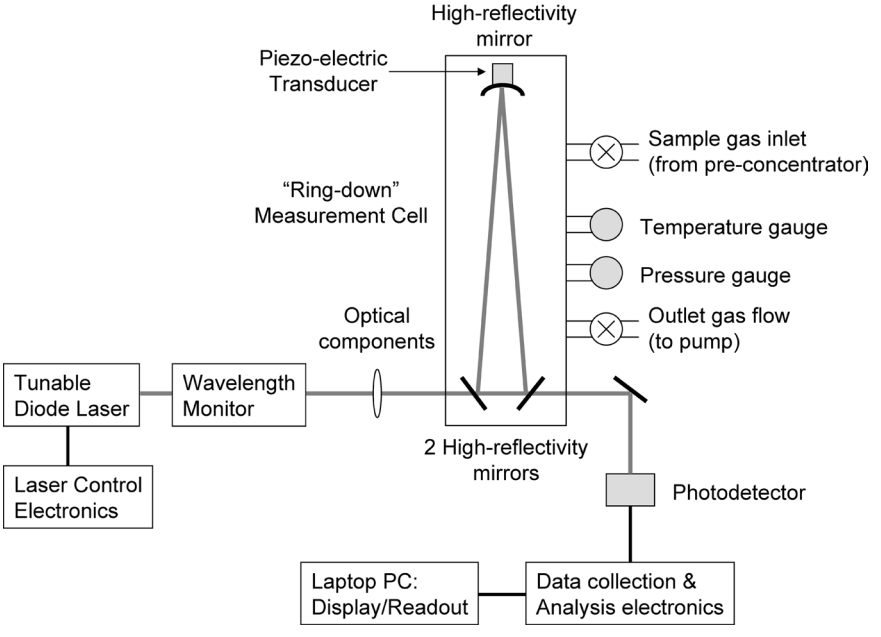

Figure 2. Schematic diagram of cavity ring-down instrument.

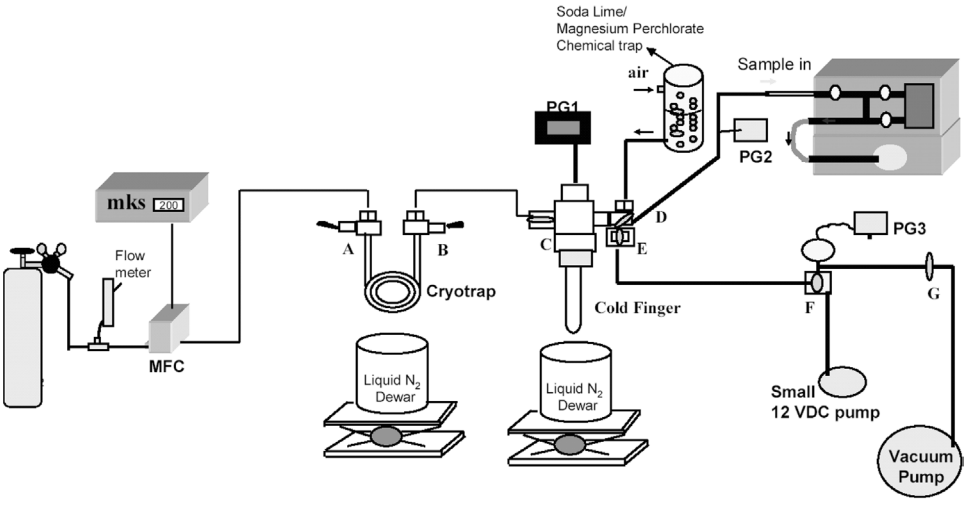

Figure 3. Schematic diagram of pre-concentration system. The diagram shows gas from a cylinder passing through a mass flow controller made by MKS instruments. The gas then passes through a pre-concentrator (inlet A, outlet B) followed by a cold finger (inlet C). The concentrated sample can then pass through a chemical trap (point D) into the measurement instrument or be directed to the vacuum line (point E). The vacuum line is driven by a small DC pump (point F) and a larger vacuum pump (point G). All portions of the flow line can be purged at any time using purge gas sources.

We mounted the optomechanical platform with vibration isolators in a thermally controlled enclosure. Then we integrated this enclosure into a 3U (5.25 in. high) rack. This enclosure also contained sample-handling valves and electronics boards. Power supplies and a vacuum pump were housed in a second 3U rack. The total weight of the instrument was ∼27 kg. The instrument was controlled using a laptop computer, which also stored the data.

Because the instrument used weak, near-infrared overtone transitions of CO_2 at 1.6 μm, it required at least a 4 % CO_2 concentration in order to achieve the target precision. Therefore, the Bowling group at the University of Utah developed and constructed a cryogenic CO_2 pre-concentrator to provide 4 % CO_2 in air samples to the CRDS instrument. The system uses stainless steel traps immersed in liquid nitrogen and requires manual operation of valves. A mass flow controller maintained sampling flow at 200 sccm, and samples were collected for 8–10 min. The condensed CO_2 was allowed to expand in a cold finger where it was re-condensed by cooling with liquid nitrogen. After evacuating any uncondensed gases, air was added to the CO_2 in the cold finger until the pressure became equal to the atmospheric pressure. The prepared sample was injected into the CRDS instrument for analysis. The concentration of CO_2 was computed by dividing the pressure of CO_2 in the cold finger prior to addition of room air by the atmospheric pressure. The final CO_2 concentration was ∼4 %. Figure 3 illustrates the pre-concentration system.

4. Results and analysis

We first present results of optical performance tests made on the CRDS system, which ultimately determine the overall instrument capability for measuring isotopes. Good performance requires a high quality cavity and wavelength monitor, excellent temperature and pressure stability, and optical measurement reproducibility. We then present results for four instrument

performance parameters that are important for isotopic applications. These parameters are precision, accuracy, memory, and measurement time.

Precision is the repeatability of a measurement, defined by the standard deviation of a set of repeated measurements of the same unknown, whereas accuracy is the ability to determine the exact concentration, defined by the standard deviation of the difference between a set of measured concentrations and the known reference standard concentration. Memory effects occur when a measurement outcome is affected by the sample history. The instrument must therefore be able to purge the previous sample adequately. Measurement time is the total time taken by the instrument to input the sample, measure the isotopic composition, and flush out the sample. Once a sample is inserted, the instrument takes multiple absorption spectra and computes the $^{13}CO_2/^{12}CO_2$ isotopic ratio from each spectrum. Each measured isotopic ratio value is called a 'scan'. The 'sample' isotopic ratio is then calculated as the average value of the isotopic ratio scans.

4.1 *CRDS system optical performance*

The attainable isotopic measurement performance of a CRDS instrument depends on the following critical optical performance parameters:

- the empty cavity ring-down time;
- the shot-to-shot variation in the measured ring-down time;
- the precision of the laser wavelength setting and monitoring;
- the ring-down system repetition rate;
- the system temperature stability;
- the cavity pressure measurement precision.

We performed a series of tests in order to measure these performance parameters and benchmark the CRDS system.

The instrument had empty cavity lifetimes exceeding 34 μs and shot-to-shot fluctuations of 0.025 %. The equivalent single-shot measurement uncertainty was $\sim 2.5 \times 10^{-10}\,\mathrm{cm}^{-1}$. Over a several minute timescale, the variation in ring-down times was nearly random, as shown by a plot of the Allan variance in figure 4. The measurement signal-to-noise ratio improved as the square-root of the number of measurements. For an average of 40 measurements per spectral point, we achieved a precision of approximately 1 part in 25,000, corresponding to a loss measurement of $4.0 \times 10^{-11}\,\mathrm{cm}^{-1}$.

Unfortunately, owing to the etaloning in the system, we were unable to fully exploit the design improvement gains in sensitivity as expected. The instrument had a long period baseline ripple of $\sim 10^{-9}\,\mathrm{cm}^{-1}$ with an ~17–34 GHz period. This ripple was easily corrected by the data-fitting algorithms. In addition, the baseline had a small short-period baseline ripple of $3 \times 10^{-11}\,\mathrm{cm}^{-1}$ with a 2–5 GHz period. This 'fast' ripple was difficult to correct in the data fitting but was small enough that it did not significantly impact the instrument precision. Further work showed that this etaloning effect was caused by poor surface quality on the mirrors and very high order cavity mode effects. It has been subsequently virtually completely eliminated. Today, we can make even faster measurements, gaining almost another order of magnitude in sensitivity. The results presented here, however, were taken on the older CRDS system.

The wavelength monitor measurements at a fixed spectral point had a standard deviation of 3 MHz, including noise in measuring and setting the laser wavelength. The wavelength monitor had a temperature fluctuation of 2–3 mK. We found that noise in the wavelength measurement was the largest contributor to fluctuations in the isotopic ratio measurements, because wavelength measurement noise distorted the measured absorption peak. By measuring

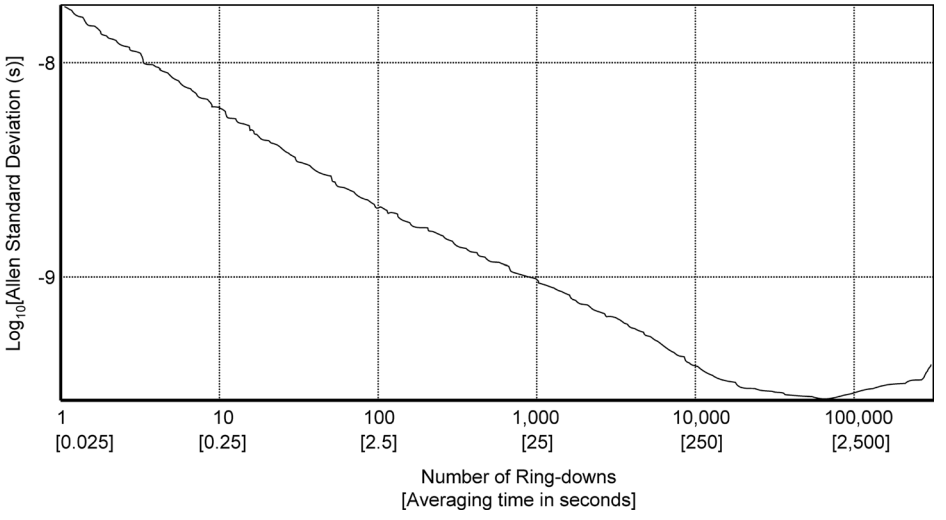

Figure 4. Plot of the Allan variance over a several-minute timescale, showing the variation in ring-down times as a function of number of samples taken or averaging time period. The variation is nearly random.

enough points around the absorption peak and averaging the peak heights from multiple scans, we reduced the impact of wavelength noise.

Each ring-down waveform was fitted using a fast algorithm similar to that published by Halmer *et al.* [20]. The measurement repetition rate was ∼40 ring-downs per second and was limited by the PZT sweep times required to accommodate the shot-to-shot variations in the laser wavelength. These variations were a result of directly modulating the laser diode when compared with using an external acousto-optic modulator. Improvements to the wavelength monitor and control circuitry could further reduce these wavelength variations and increase the measurement repetition rate.

The thermal control system maintained the temperature of the optomechanical platform. Figure 5a shows a plot of the optomechanical temperature (measured at the RDC wall, which was taken as a proxy for the sample gas temperature) over a period of 117 h of continuous operation of the prototype in a laboratory environment. Each data point represents an average

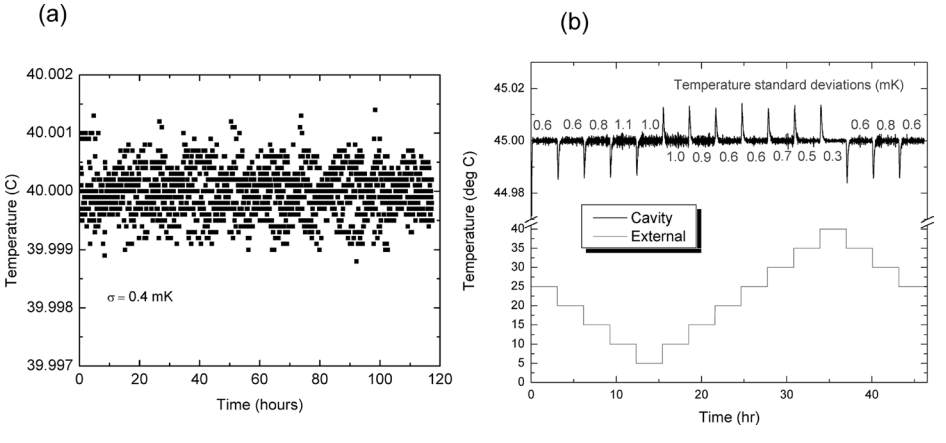

Figure 5. Temperature performance of CRDS instrument: (a) cavity temperature when external temperature is at room temperature and (b) cavity temperature when varying ambient temperature from 5 to 40 °C.

over a 5 min measurement. The standard deviation in temperature over 117 h was 0.4 mK. Figure 5b shows the response of the thermal control system, as measured on the ring-down system in an environmental chamber, to changes in external temperature. At temperatures between 5 and 40 °C, the control system maintained the temperature with a precision of better than 1.1 mK standard deviation and a maximum step excursion not exceeding 20 mK. The isotopic ratio measurement depends on the cavity temperature at a rate of −18 ‰/K, so the cavity temperature fluctuations contributed only 0.02 ‰ to the measurement error of the instrument.

A pressure transducer measured the cavity pressure to a precision of better than 13.4 Pa. The system electronics used this pressure measurement to correct for changes in the cavity pressure during measurements. An uncertainty of 13.4 Pa in pressure corresponds to a 1 part in 16,000 uncertainty in the measured carbon dioxide concentration at 380 ppm (atmospheric concentration). Cavity leak rates were <4 Pa/h. The measurements were performed at ∼6.7 kPa and were, therefore, not significantly contaminated by leakage during the measurement time. Figure 6 shows the pressure reproducibility of the system.

The advanced prototype instrument was calibrated to convert the measured $^{13}CO_2$ to $^{12}CO_2$ peak height ratios into delta values. The calibration was performed using known isotopic ratio standards from Cambridge Isotope Laboratories (CIL) to determine the absolute scale at fixed pressure, total CO_2 concentration, and temperature. Corrections to the calibration between peak height ratio and delta value were determined for changes in sample pressure, sample concentration, RDC temperature, and ring-down engine module internal temperature.

The peak height ratio varied by a change in delta value of 0.0045 ‰/Pa. We measured the sample pressure with a precision of better than 13.4 Pa, resulting in <0.06 ‰ error in the delta measurement.

The dependence of peak height ratio on total CO_2 concentration was equivalent to a delta dependence of 0.7 ‰/(%CO_2). Using the $^{12}CO_2$ peak height, we were easily able to measure the CO_2 concentration to better than 0.01 %, resulting in no significant contribution to the measurement error from the total CO_2 concentration level.

The peak height ratios varied with cavity temperature at a rate which was equivalent to a delta variation of 18 ‰/°C. Our instruments demonstrated an RMS temperature stability of

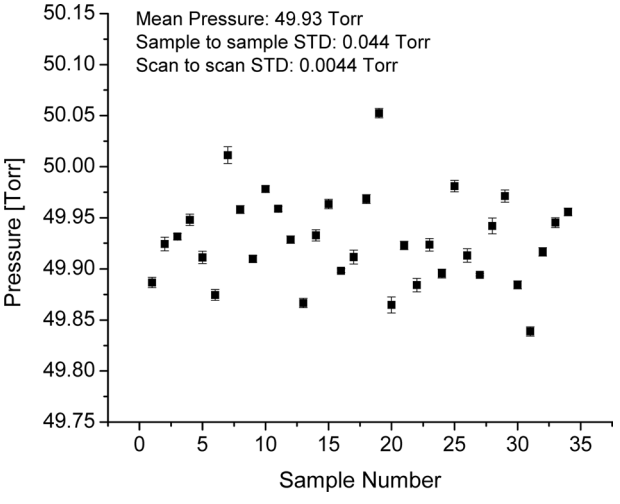

Figure 6. Variation of sample pressure in CRDS instrument over a set of 35 samples.

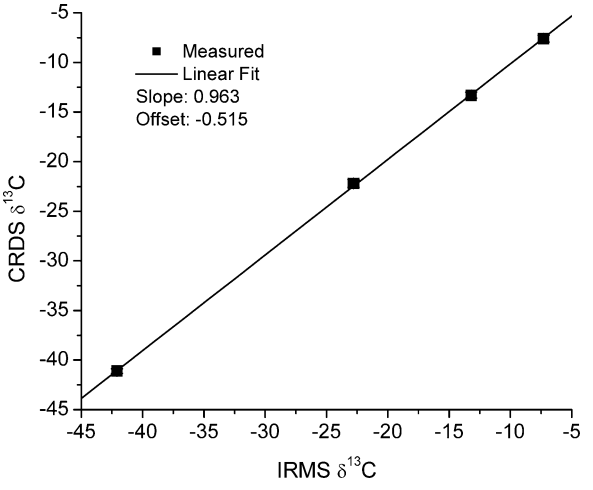

Figure 7. Calibration curve of CRDS instrument using four different δ^{13}C bottles. Only two bottles were from CIL.

1 mK, so the RMS cavity temperature contribution to the measurement error was estimated to be only 0.02 ‰.

The peak height ratio depended on the air temperature, as measured by a sensor inside the ring-down engine module, at a rate equivalent to a delta variation of 0.1 ‰/°C.

Overall, we demonstrated that the cumulative errors in the instrument produce an expected error of <0.14‰. Thus, our target precision of 0.2‰ was deemed to be achievable. Figure 7 illustrates the linearity of the system for four different δ^{13}C values ranging from −42.3 to −7.3 ‰. Note that many samples were measured at each δ^{13}C value to estimate the instrument precision and linearity.

4.2 *CRDS system isotopic measurement performance*

Utilizing the calibrations and correction factors for cavity pressure, CO_2 concentration, and cavity ring-down engine module temperature, the CRDS instrument was tested for sample-to-sample measurement precision at Picarro. The results are shown in figure 8, for the calibration sample with a delta level closest to the target environmental measurement application range of −7 to −15 ‰. For each sample loaded into the RDC, the absorption spectrum was measured 10 times. The average scan time was ∼8 min. The delta value was determined for each spectral scan and averaged to produce a 'sample' value. The error bars in figure 7 show the standard deviation in the isotopic ratio 'scan' value, for sets of 10 measurements, is 0.3 ‰ on average. The standard deviation of the 20 'sample' values measured was 0.12 ‰ (which is lower than the 'scan' standard deviation because each 'sample' value is an average of 10 scan values). The time to perform a single sample measurement was ∼78 min. The precision of the sample values exceeded the performance target of 0.2 ‰.

Tests of instrument precision, accuracy, and memory were performed independently by the Bowling group at the University of Utah. Three types of lab experiments were performed. In each, the CRDS instrument was optimized to measure repeated 'samples', with each sample consisting of five separate measurements (called 'scans') of an initial gas sample from the tank. Each scan took 7.5–8 min, with a single sample taking roughly 40 min. The time to fill the cell with each new sample and stabilize its temperature added another 7.5 min to each

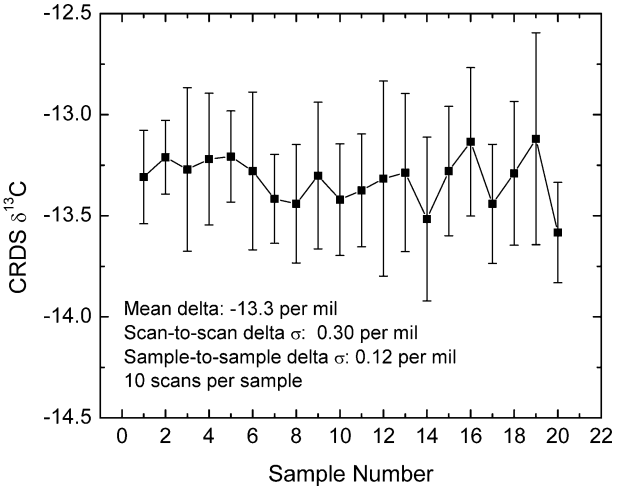

Figure 8. Set of 20 measurements on calibration sample with a delta level of −13 ‰ illustrated the CRDS instrument precision. For each sample, 10 scans of the absorption spectrum were made to determine the delta value and then averaged. Error bars represent the standard deviation of the each set of 10 scans.

scan. Thus, the total measurement time for each sample was ∼78 min. A collection of multiple 'samples' in this article is referred to as a 'run'.

A consistent problem was identified with the first sample in each run, regardless of experiment type. The first sample measured always had an incorrect $\delta^{13}C$ and low CO_2 concentration (the CRDS does report this even though the instrument was not optimized to measure it). Early experiments identified this problem as a sample-transfer issue and it was not resolved. Hence, the first sample from each run was omitted in the final data analysis.

The first experiment used 5 % CO_2 gas samples from compressed cylinders with no cryogenic trapping, in order to test the performance of the CRDS system by itself. Three cylinders were used to generate precision and accuracy data.

- Cylinder 1 (CLM-3781-10, 5 % CO_2 in air) had a $\delta^{13}C$ of −7.30 ‰ and was calibrated by CIL using IRMS.
- Cylinder 2 was identical to Cylinder 1.
- Cylinder 3 (Utah Laboratory Tank, 5 % CO_2 in air) had a $\delta^{13}C$ of −42.30 ‰ and was calibrated by the Bowling group at Utah.

The number of samples per run (N) varied from 1 to 95. The results are shown in table 1. The accuracy varied from 0.01 to −1.63 ‰. The precision varied from 0.12 to 0.37 ‰.

The second experiment used the Utah cryogenic trapping system to pre-concentrate CO_2 from five calibration tanks. These tanks were prepared and calibrated by the Bowling group using IRMS. They varied in CO_2 concentration from 379.66 to 472.57 ppmv and in $\delta^{13}C$ from −8.43 to −16.00 ‰. The concentrated sample (∼4 % CO_2) was measured using the CRDS system. The number of samples per run varied from 3 to 27. The results are shown in table 2. The standard deviation of each run varied from 0.14 to 0.96 ‰, but was usually <0.25 ‰. On the basis of these results, we estimated the mean precision of the combined CRDS and cryotrap system to be 0.2 ‰. It should also be noted from table 2 that the CRDS $\delta^{13}C$ measurements were consistently more negative than the known tank $\delta^{13}C$ values. Figure 9a illustrates the consistent negative bias between the reference and CRDS data. The linearity of the plot indicated that CRDS measurements have the potential to be calibrated, in order to match the IRMS reference.

Table 1. Results from experiments at the University of Utah comparing CRDS and IRMS performance for 5 % CO_2 samples from a cylinder with no pre-concentration.

Experiment	*N*	Cyl (number)	Delta^{13}C Avg (‰)	Delta^{13}C Std Dev (‰)	CO_2 conc. Avg (%)	CO_2 conc. Std Dev (%)	Delta^{13}C Known (‰)	Deviation (‰)
Cambridge 1	17	1	−6.35	0.14	4.39	0.02	−7.30	−0.95
Cambridge 2	1	1	−6.54	0.72	1.66	0.01	−7.30	−0.76
Cambridge 3	38	1	−7.31	0.36	4.42	0.01	−7.30	0.01
Cambridge 4	9	1	−7.44	0.15	4.41	0.00	−7.30	0.14
Cambridge 5	9	1	−7.66	0.37	4.42	0.01	−7.30	0.36
Cambridge 6	49	1	−7.53	0.25	4.41	0.02	−7.30	0.23
Cambridge 7	95	2	−7.89	0.19	4.33	0.02	−7.30	0.59
Utah 1	23	3	−40.73	0.16	4.89	0.12	−42.30	−1.57
Utah 2	74	3	−40.67	0.14	4.97	0.01	−42.30	−1.63
Utah 3	17	3	−40.74	0.12	4.97	0.01	−42.30	−1.56
Picarro	6	2	−7.6	0.15	4.43	0.01	−7.30	0.30

The third experiment attempted to compare CRDS directly with IRMS over a wide dynamic range by co-measurement of air samples collected from the roof of the Bowling laboratory. A sample was collected via CRDS with the cryogenic trapping system, and simultaneously, an air sample was collected in a flask for subsequent analysis by IRMS. Data obtained are presented in table 3 and plotted in figure 9b. The comparison was poor, due to the sample-transfer problem identified earlier. The CRDS required repeated samples to achieve stable results, and because there was only a single sample available in this configuration, the measurements do not match well. These results indicate that for any CRDS system that cannot directly measure the CO_2 sample, namely one that requires pre-concentration, frequent calibration is necessary, in order to maintain accuracy of the system.

Table 2. Results from experiments at the University of Utah comparing CRDS and IRMS performance for environmental CO_2 samples from a reference tank with cryotrap pre-concentration to 5 % CO_2.

Experiment	*N*	Delta^{13}C Avg (‰)	Delta^{13}C Std Dev (‰)	CO_2 conc. (Prior conc.) (ppmv)	CO_2 conc. Avg (%)	CO_2 conc. Std Dev (%)	Delta^{13}C Known (‰)	Deviation (‰)
Cryotrap Expt 1	5	−8.04	0.48	379.66	5.22	0.75	−8.43	−0.39
Cryotrap Expt 2[†]	11	−8.07	0.96	379.66	5.08	0.90	−8.43	−0.36
Cryotrap Expt 2[†]	11	−9.74	0.92	379.66	4.83	1.33	−8.43	1.31
Cryotrap Expt 3	23	−8.55	0.33	379.66	5.64	0.11	−8.43	0.12
Cryotrap Expt 4	3	−9.33	0.48	379.66	3.91	0.16	−8.43	0.90
Cryotrap Expt 5	11	−8.58	0.24	379.66	3.7	0.93	−8.43	0.15
Cryotrap Expt 6	4	−8.75	0.25	379.66	3.98	0.21	−8.43	0.32
Cryotrap Expt 7	14	−10.28	0.2	421.01	4.5	0.04	−10.02	0.26
Cryotrap Expt 9	10	−16.26	0.27	472.57	4.9	0.05	−16.00	0.26
Cryotrap Expt 12	11	−9.92	0.24	395.06	4.13	0.04	−9.41	0.51
Cryotrap Expt 13	9	−9.58	0.19	472.41	4.78	0.41	−8.89	0.69
Cryotrap Expt 14	16	−16.46	0.22	472.57	5.05	0.03	−16.00	0.46
Cryotrap Expt 15	21	−10.75	0.31	421.01	4.45	0.04	−10.02	0.73
Cryotrap Expt 16	16	−9.69	0.23	472.41	4.97	0.12	−8.89	0.80
Cryotrap Expt 17	27	−10.26	0.39	395.06	4.15	0.05	−9.41	0.85
Cryotrap Expt 18	19	−16.43	0.25	472.57	5.05	0.06	−16.00	0.43
Cryotrap Expt 19	6	−10.54	0.25	421.01	4.47	0.01	−10.02	0.52
Cryotrap Expt 20	21	−10.40	0.17	421.01	4.46	0.03	−10.02	0.38
Cryotrap Expt 21	22	−9.44	0.14	472.41	4.97	0.06	−8.89	0.55
Cryotrap Expt 22	18	−9.91	0.14	395.06	4.13	0.03	−9.41	0.50

[†]The temperature of the cryotrap was 20 degrees higher than normal.

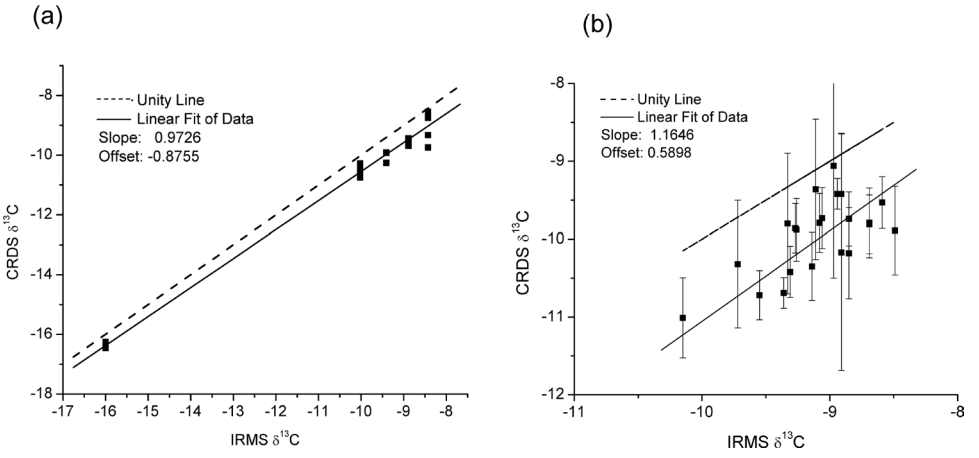

Figure 9. (a) Comparison between CRDS and IRMS measured values of δ^{13}C for four different reference samples obtained from reservoir tanks at the University of Utah and (b) comparison between CRDS and IRMS measured values of δ^{13}C for roof air samples taken at the University of Utah laboratory.

Table 3. Results from experiments at the University of Utah comparing CRDS and IRMS performance for environmental CO_2 samples from roof air with cryotrap pre-concentration to 4 % CO_2.

Experiment	*N*	Delta^{13}C Avg (‰)	Delta^{13}C Std Dev (‰)	CO_2 conc. Avg (‰)	Delta^{13}C IRMS (‰)	Deviation (‰)
Roof Air 1	1	−9.86	0.32	3.67	−9.27	0.59
Roof Air 2	1	−9.74	0.35	3.80	−8.85	0.89
Roof Air 3	1	−9.88	0.40	3.99	−9.26	0.62
Roof Air 4	1	−9.89	0.57	3.87	−8.49	1.40
Roof Air 5	1	−9.81	0.38	3.8	−8.69	1.12
Roof Air 6	1	−10.32	0.82	3.74	−9.72	0.60
Roof Air 7	1	−11.01	0.52	4.07	−10.15	0.86
Roof Air 8	1	−10.35	0.44	3.95	−9.14	1.21
Roof Air 9	1	−10.18	0.59	3.83	−8.85	1.33
Roof Air 10	1	−9.42	0.78	3.73	−8.91	0.51
Roof Air 11	1	−9.42	0.20	3.9	−8.94	0.48
Roof Air 12	1	−9.06	1.44	4.12	−8.97	0.09
Roof Air 13	1	−10.17	1.52	4.26	−8.91	1.26
Roof Air 14	1	−9.36	0.90	3.69	−9.11	0.25
Roof Air 15	1	−10.72	0.32	3.92	−9.55	1.17
Roof Air 16	1	−10.69	0.20	3.97	−9.36	1.33
Roof Air 17	1	−9.79	0.38	4.12	−9.08	0.71
Roof Air 18	1	−9.73	0.39	4.22	−9.06	0.67
Roof Air 19	1	−9.79	0.45	3.76	−8.69	1.10
Roof Air 20	1	−9.53	0.33	3.76	−8.59	0.94
Roof Air 21	1	−9.80	0.90	3.68	−9.33	0.47

5. Conclusions

The plumbing system for sample transfer to the CRDS has subsequently been redesigned to alleviate the sample-transfer problem. For this early work, the sampling problem prevented suitable measurement of unknown samples. Overall, the CRDS system showed good precision (often better than 0.2 ‰) for 4 % CO_2 and, with cryotrapping, also had good precision (0.15–0.25 ‰) for ambient CO_2. The measurement time required to achieve this precision was ∼78 min. There are a variety of applications that such a CRDS instrument might be suited for

with this precision at higher CO_2 concentrations (*i.e.* 5–10 %), such as medical human breath analysis or animal breath experiments.

The precision of CRDS for ambient CO_2 concentrations (300–400 ppmv) was not as good as MS, which is presently 0.05 ‰ in many laboratories. A different spectral region for analysis was subsequently selected, in order to measure lower concentrations of CO_2, specifically down to 1 % CO_2 for small animal studies, and will be reported elsewhere. This improvement reduces the requirements and associated fractionation issues for pre-concentration. The advent of commercially available, reliable 2.1 μm DFB diode lasers, providing access to absorption lines that are 60 times stronger than at 1.6 μm, should allow direct measurement of environmental concentrations of CO_2 with the same precision achieved in this study. With improved mirrors and cavity designs to minimize etalon effects, and internally designed electronics optimized for CRDS data acquisition, we have currently been able to reduce the measurement time to ∼5 min for the same precision. These recent results will be reported elsewhere.

The accuracy of the CRDS system without calibration was not sufficient for high-quality measurements. However, the instrument was quite linear, and with frequent measurement of suitable calibration gases, CRDS is likely to provide excellent results.

Small size, robust design, and potential for frequent measurements at a remote site make CRDS technology attractive for remote atmospheric measurement applications. Future experiments need to determine the long-term stability of the instrument, in order to minimize the variability in the mean $\delta^{13}C$ measured on separate multi-sample runs of the same sample. The ultimate test of the instrument will be made directly in field applications.

An observation has been made [10] that the adoption of laser spectroscopy to replace traditional IRMS is a 'chicken-and-egg' problem, wherein the technology will be adopted once it is mature, but it cannot mature until it is adopted by the international isotope community. In recent years, commercial isotope measurement systems using lead-salt [21] mid-infrared lasers have become available. The use of these instruments [21, 22] by the isotope community demonstrates a willingness to consider laser spectroscopy as a real alternative to IRMS. These mid-infrared systems, however, suffer from the same portability and price limitations as IRMS. It is our hope that with the advent of reliable 2 μm diode lasers, near-infrared CRDS technology can resolve both of these limitations and improve in sensitivity to make direct isotopic measurements of atmospheric CO_2 concentration, thereby succeeding in becoming widely used for isotopic measurements in scientific applications.

Acknowledgements

The authors at Picarro would like to thank the Department of Energy (DOE), which has made this work possible through their SBIR grant program (Grant no. DE-FG03-01ER83250). This support does not constitute an endorsement by the DOE of the views expressed in this article. The authors would also like to thank Richard Zare and Marc Levenson for their support and guidance over the past 2 years.

References

[1] P.P. Tans, J.A. Berry, R.F. Keeling. Oceanic $^{13}C/^{12}C$ observations – a new window on ocean CO_2 uptake. *Global Biogeochem. Cycles*, **7**, 353–368 (1993).

[2] I.G. Enting, C.M. Trudinger, R.J. Francey. A synthesis inversion of the concentration and $\delta^{13}C$ of atmospheric CO_2. *Tellus B*, **47**, 35–52 (1995).

[3] P. Ciais, P. Friedlingstein, D.S. Schimel, P.P. Tans. A global calculation of the $\delta^{13}C$ of soil respired carbon: implications for the biosphere uptake of anthropogenic CO_2. *Global Biogeochem. Cycles*, **13**, 519–530 (1999).

[4] D.R. Bowling, D.D. Baldocchi, R.K. Monson. Dynamics of isotopic exchange of carbon dioxide in a Tennessee deciduous forest. *Global Biogeochem. Cycles*, **13**, 903–922 (1999).

[5] D. Bowling, N. McDowell, B. Bond, B. Law, J. Ehleringer. ^{13}C content of ecosystem respiration is linked to precipitation and vapor pressure deficit. *Oecologia*, **131**, 113–124 (2002).
[6] D.R. Bowling, P.P. Tans, R.K. Monson. Partitioning net ecosystem carbon exchange with isotopic fluxes of CO_2. *Glob. Change Biol.*, **7**, 127–145 (2001).
[7] J.B. Miller, P.P. Tans, J.W.C. White, T.J. Conway, B.W. Vaughn. The atmospheric signal of terrestrial carbon isotopic discrimination and its implication for partitioning carbon fluxes. *Tellus B*, **55**, 197–206 (2003).
[8] C.D. Keeling. The concentration and isotopic abundances of atmospheric carbon dioxide in rural areas. *Geochim. Cosmochim. Acta*, **13**, 322–334 (1958).
[9] G. Berden, R. Peeters, G. Meijer. Cavity ring-down spectroscopy: experimental schemes and applications. *Int. Rev. Phys. Chem.*, **19**, 565–607 (2000).
[10] E.R.T. Kerstel. Isotope ratio infrared spectrometry. In *Handbook of Stable Isotope Analytical Techniques*, Pier de Groot (Ed.), Vol. I, Chapter 34, pp. 759–787, Elsevier, Amsterdam (2004).
[11] T.G. Spence, C.C. Harb, B.A. Paldus, R.N. Zare, B. Willke, R.L. Byer. A laser-locked cavity ring-down spectrometer employing an analog detection scheme. *Rev. Sci. Inst.*, **71**, 347–353 (2000).
[12] G. Gagliardi, A. Castrillo, R.Q. Iannone, E.R.T. Kerstel, L. Gianfrani. High-precision determination of the $^{13}CO_2/^{12}CO_2$ isotope ratio using a portable 2.008 μm diode-laser spectrometer. *Appl. Phys. B*, **77**, 119–124 (2003).
[13] D.R. Bowling, S.D. Sargent, B.D. Tanner, J.R. Ehleringer. Tunable diode laser absorption spectroscopy for stable isotope studies of ecosystem-atmosphere CO_2 exchange. *Agr. Forest Meteorol.*, **118**, 1–19 (2003).
[14] E.R.T. Kerstel, G. Gagliardi, L. Gianfrani, H.A.J. Meijer, R. van Trigt, R. Ramaker. Determination of the $^2H/^1H$, $^{17}O/^{16}O$, and $^{18}O/^{16}O$ isotope ratios in water by means of tunable diode laser spectroscopy at 1.39 μm. *Spectrochim. Acta A*, **58**, 2389–2396 (2002).
[15] L. Gianfrani, G. Gagliardi, G.M. van Burgel, E.R.T. Kerstel. Isotope analysis of water by means of near infrared dual-wavelength diode laser spectroscopy. *Opt. Express*, **11**, 1566–1576 (2003).
[16] K. Uehara, K. Yamamoto, T. Kikugawa, N. Yoshida. Isotope analysis of environmental substances by a new laser-spectroscopic method utilizing different pathlengths. *Sens. Actuators B*, **74**, 173–178 (2001).
[17] K. Uehara, K. Yamamoto, T. Kikugawa, S. Toyoda, K. Tsuji, N. Yoshida. Precise isotope abundance ratio measurement of nitrous oxide using diode lasers. *Sens. Actuators B*, **90**, 250–255 (2003).
[18] H. Dahnke, D. Kleine, W. Urban, P. Hering, M. Mürtz. Isotopic ratio measurement of methane in ambient air using mid-infrared cavity leak-out spectroscopy. *Appl. Phys. B*, **72**, 121–125 (2001).
[19] E.R. Crosson, K.N. Ricci, B.A. Richman, F.C. Chilese, T.G. Owano, R.A. Provencal, M.W. Todd, J. Glasser, A.A. Kachanov, B.A. Paldus, T.G. Spence, R.N. Zare. Stable isotope ratios using cavity ring-down spectroscopy: determination of $^{13}C/^{12}C$ for carbon dioxide in human breath. *Anal. Chem.*, **74**, 2003–2007 (2002).
[20] D. Halmer, G. von Basum, P. Hering, M. Mürtz. Fast exponential fitting algorithm for real-time instrumental use. *Rev. Sci. Instrum.*, **75**, 2187–2191 (2004).
[21] D.R. Bowling, S.D. Sargent, B.D. Tanner, J.R. Ehleringer. Tunable diode laser absorption spectroscopy for stable isotope studies of ecosystem-atmosphere CO_2 exchange. *Agr. Forest Meteorol.*, **118**, 1–19 (2003).
[22] T.J. Griffis, J.M. Baker, S.D. Sargent, B.D. Tanner, J. Zhang. Measuring field-scale isotopic CO_2 fluxes with tunable diode laser absorption spectroscopy and micrometeorological techniques. *Agr. Forest Meteorol.*, **124**, 15–29 (2004).